Effect of Backfill Relative Density on Lateral Response of a Bridge Abutment Wall

A. Lemnitzer
University of California, Irvine, USA

C. Hilson, E. Taciroglu, J.W. Wallace & J.P. Stewart
University of California, Los Angeles, USA

SUMMARY:
Three abutment backwall systems with dimensions of 4.57 m in width, 2.8m in height, and 0.91m in thickness were subjected to lateral loading into a silty sand backfill with 1.68m and 2.4m heights. The backfill material was placed and compacted using vibratory methods in the field. Lateral loading was applied under displacement control while restraining the wall from vertical uplift. The tests were performed against a reaction block under quasi-static conditions up to displacements equal to 15% of the wall height, with unloading and reloading at several displacement levels. The backfill was prepared to different relative densities for the two tests having 2.4 m backfill height, which strongly affected the stiffness and capacity of the wall-soil system under lateral loading. The predictability of the performance is investigated using numerical simulations that apply the results of extensive laboratory testing of the backfill materials.

Keywords: Passive Earth Pressure, Bridge Abutment, Lateral Loading

1. INTRODUCTION

Bridge structures are typically constructed with earth abutments at their ends. Important components of bridge abutments include a backwall, two wingwalls, a support foundation below the backwall and compacted backfill material. As a bridge deck is shaken by an earthquake, its longitudinal response causes the end of the deck to strike the backwall, which in turn engages the backfill soil. Accordingly, a major source of lateral load resistance and energy dissipation due to longitudinal shaking of the bridge deck is provided by the nonlinear passive response of the backwall-backfill system. The load-deflection behavior of abutment walls up to the point of passive failure has been investigated with experiments and analytical simulations (e.g. Romstadt *et al.*, 1995; Rollins, 2006; Lemnitzer *et al.*, 2009; Shamsabadi *et al.*, 2007, 2010). Current California Seismic Design Criteria (SDC, 2010) are based on two field experiments on cohesive (Romstadt *et al*. 1995) and granular (Lemnitzer *et al*. 2009) backfill materials.

The experimental work presented in this paper was performed at the UCLA-Caltrans test site in Hawthorne, CA, and involved two 2.4 m backfills referred to as $T_{2.4,1}$ and $T_{2.4,2}$ (completed in 2009 and 2010, see Stewart *et al.* 2011) and one 1.68 m backfill referred to as $T_{1.68}$ (completed in 2006, published by Lemnitzer *et al.* 2009). Table 1.1 summarizes the various backwall tests undertaken at this test site. This paper focuses on the two 2.4 m specimens, which utilized different vibratory procedures for backfill compaction, achieving different in situ relative densities.

Table 1.1. Overview of Tested Backfill Systems

Test ID	Backfill Height [m]	Test Completed	Compaction Method
$T_{1.68}$	1.68	07/2006	Vibratory Plate & Small Handwhacker
$T_{2.4,1}$	2.4	07/2009	Large Vibratory Roller
$T_{2.4,2}$	2.4	12/2010	Vibratory Plate & Small Handwhacker

2. OVERVIEW OF THE LARGE SCALE TEST PROGRAM

The test specimens consisted of a backwall with dimensions of 2.68 m in height (the lower 2.4 m of which retained backfill), 4.57 m in width, and 0.91 m in thickness. The backwall rested on the natural ground (in $T_{1.68}$ and $T_{2.4,1}$) or on a steel plate with intermediate grout between the irregular base concrete surface and the plate ($T_{2.4,2}$). A reaction block with a loading capacity of 13.3 MN in the linear range, founded on two 1.83 m diameter reinforced concrete piles was located at a clear distance of 2.9 m from the abutment wall to provide the lateral resistance needed to push the test specimen into the adjacent backfill material. Hydraulic actuators were installed between the backwall and the reaction block in horizontal and diagonal configurations to apply lateral displacements and prevent the backwall from vertical uplift during testing. As shown in Figure 2.1 and 2.2, natural soils behind the backwall were excavated to 0.6 m below the wall. Wingwalls were simulated using 2.5 cm thick plywood sheathing erected approximately 0.3 m from both sides of the backwall, and braced with stakes anchored into the adjacent native slopes (Figure 2.1). The plywood was furnished with layers of PVC foil to minimize friction between the sidewalls and the backfill material. During backfill compaction, material was also placed and compacted behind the wingwalls to minimize bulging or displacement of the plywood.

Figure 2.1. Photograph of backwall specimen during construction

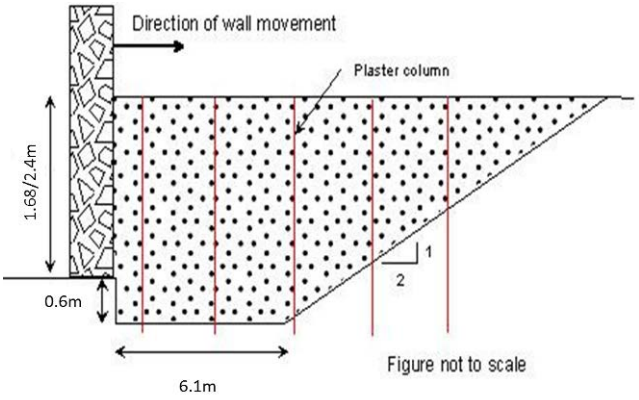

Figure 2.2. Section view of test specimen

Test specimens were equipped with five linear voltage differential transducers (LVDTs). Three horizontally aligned LVDTs were used to measure and control the individual and average horizontal displacement of the wall into the backfill material. Two vertical LVDTs were placed on top of the wall and rested on smooth steel plates to record/control to zero the potential vertical uplift of the wall. Testing was performed under quasi static loading with a loading rate of about 0.2 inch/min and smaller. Displacements were applied in small increments and unloading-reloading cycles were conducted at selected displacement levels. Unloading cycles were minimal in displacement magnitude and did not allow for soil gapping.

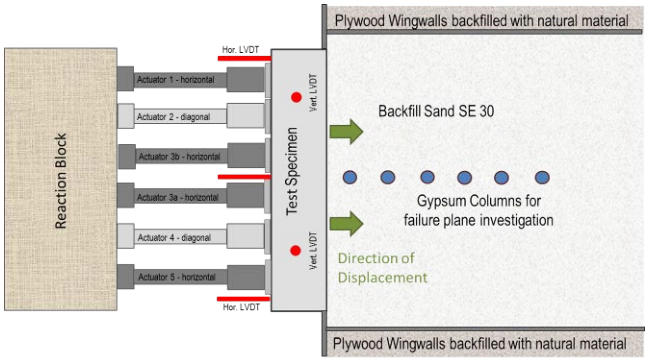

Figure 2.3 Schematic plan view of test specimen

Figure 2.4. Photograph of loading system in the field

Figure 2.5. shows the measured passive load displacement relationships for all three abutment-backfill tests. It can be seen that $T_{1.68}$ and $T_{2.4,2}$ have closer agreement in terms of initial stiffness and vary in ultimate passive capacity according to their backfill heights by a factor of approximately 2. When comparing the two 2.4m backfill height tests, $T_{2.4,1}$ shows a lower initial stiffness (50%) and a significantly smaller capacity (by 60%) than $T_{2.4,2}$, even though both tests were conducted under identical boundary conditions. Table 2.1 summarizes major parameters of the test results. Besides initial stiffness and ultimate passive capacity, Table 2.1 presents the normalized wall deflection at ultimate passive capacity and the passive earth pressure coefficient K_p which was calculated as:

$$K_p = \frac{2P_p}{\gamma h^2 w} \tag{2.1}$$

where P_p is the total passive force, h is the backfill height, γ the total unit weight of the soil (taken as 2.05g/cm^3) and w is the effective width of the backfill material between wingwalls (taken as 4.87 m for $T_{1.68}$ and 5.18 m for $T_{2.4,1}$ and $T_{2.4,2}$).

In this paper, we focus on the properties of the backfill material and jnvestigate the variation in the test results between the identical 2.4m backfill experiments using field and laboratory measurements of the fill sand.

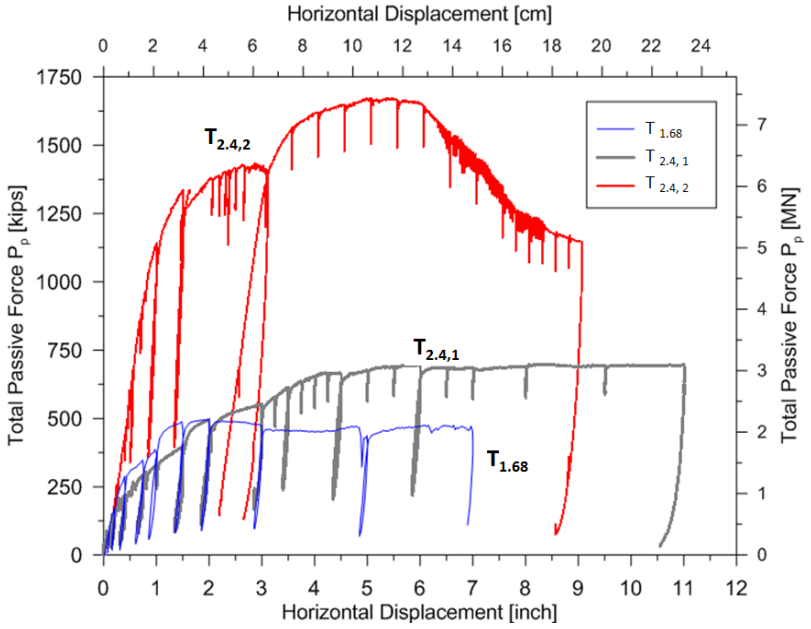

Figure 2.3. Load-displacement relationships for the abutment systems tested

Table 2.1 Overview of test results

Test ID	**Initial Stiffness** K_i [kN/cm/m]	**Ultimate Passive Capacity** P_p [kN]	**Normalized deflection at** P_p Δ_{max}/h	**Earth Pressure Coefficient Kp**
$T_{1.68}$	345	2210	0.03	16.3
$T_{2.4,1}$	239	3150	0.06	10
$T_{2.4,2}$	495	7340	0.057	24

3. SOIL PROPERTIES AND THEIR INFLUENCE

The backfill material selected for this study consisted of well-graded sand with approximately 5-10% silty fines known as SE 30 fill sand. It can be classified in the Unified Soil Classification system as SP (glean, gravelly sand) and Group A-3 (fine sand) in the AASHTO soil classification system. Laboratory tests on the material included modified Proctor compaction tests, triaxial testing, minimum and maximum density tests and sieve analysis (not presented in this manuscript). Field testing included sand cone tests on the compacted material and CPT testing following test completion.

Modified Proctor (MP) tests (ASTM D1557) were performed in the laboratory to develop compaction curves for samples from all three tests $T_{1.68}$, $T_{2.4,1}$ and $T_{2.4,2}$, with the results shown for $T_{2.4,1}$ and $T_{2.4,2}$ in Figure 3.1. Results from MP tests on backfill of specimen $T_{1.68}$ can be found in the literature (Lemnitzer *et al.*, 2009) and were in agreement with the results shown below. The MP compaction curve for this material has an optimum water content between 9 - 11% and an average dry unit weight of 1.95g/cm^3.

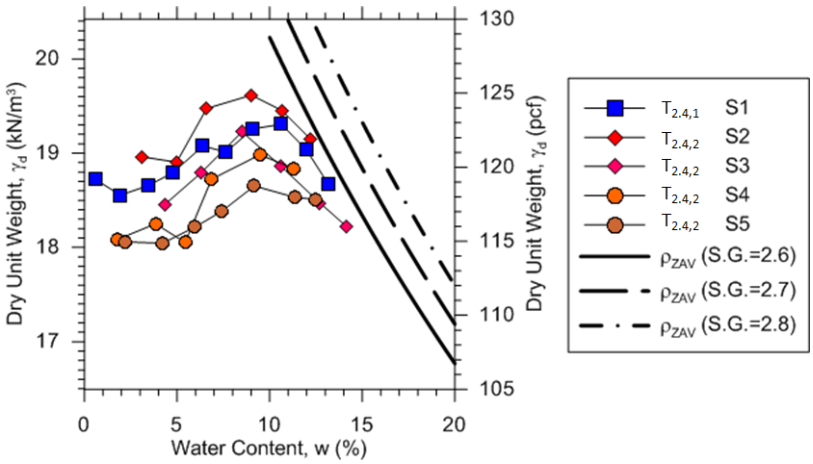

Figure 3.1. Modified Proctor compaction curves for soil samples from backfill $T_{2.4,1}$ and $T_{2.4,2}$

During specimen construction, the backfill material was placed in 30 cm lifts in $T_{1.68}$ and $T_{2.4,1}$ and 20 cm lifts in $T_{2.4,2}$. In between lifts, sand cone tests were performed to measure density and water contents per ASTM 1556. The upper 5 cm of the lift were scraped off to remove loose material and ensure a more accurate representation of the level of compaction. Results indicate MP relative compaction levels between 94% and 112%, with a mean of 96% for test $T_{1.68}$. For $T_{2.4,1}$ relative compactions between 93% and 106.8% with a mean of 98% and a standard deviation of 5.8% were measured. Compaction levels for $T_{2.4,2}$, ranged between 93% and 114.8%, with a mean of 98.6% and a standard deviation of 6.0%. As-compacted water contents are generally at or near optimum. All relative compactions were computed using a maximum dry density of 18.85 kN/m^3. Figures 3.2 and 3.3 show the two different compaction methods for $T_{2.4,1}$ and $T_{2.4,2}$ during specimen construction.

Maximum and minimum dry density experiments were performed on several bulk samples according to ASTM D4253 and ASTM D4254. The average maximum dry density of 18.1 kN/m^3 (from ASTM D4253) is lower than the MP maximum density of 18.9 kN/m^3 and the mean from the sand cone tests of 18.6 kN/m^3. This occurs because the relative density standards for maximum density do not allow grain breakage during testing, whereas grain breakage is likely to occur in the MP test and during field compaction. Therefore, in situ relative densities are difficult to evaluate in this case, but clearly they are high (near 1.0).

Figure 3.2. Compaction of backfill material with vibratory roller and hand whacker in $T_{2.4,1}$

Figure 3.3. Compaction of backfill material with vibratory plate and hand whacker in $T_{2.4,2}$.

In order to gain further insight in the influence of compaction method, lift thickness and compaction uniformity throughout the backfill material, cone penetration tests (CPT) were conducted after test completion of $T_{2.4,1}$ and $T_{2.4,2}$ at various locations in the backfill soil and revealed the following results:

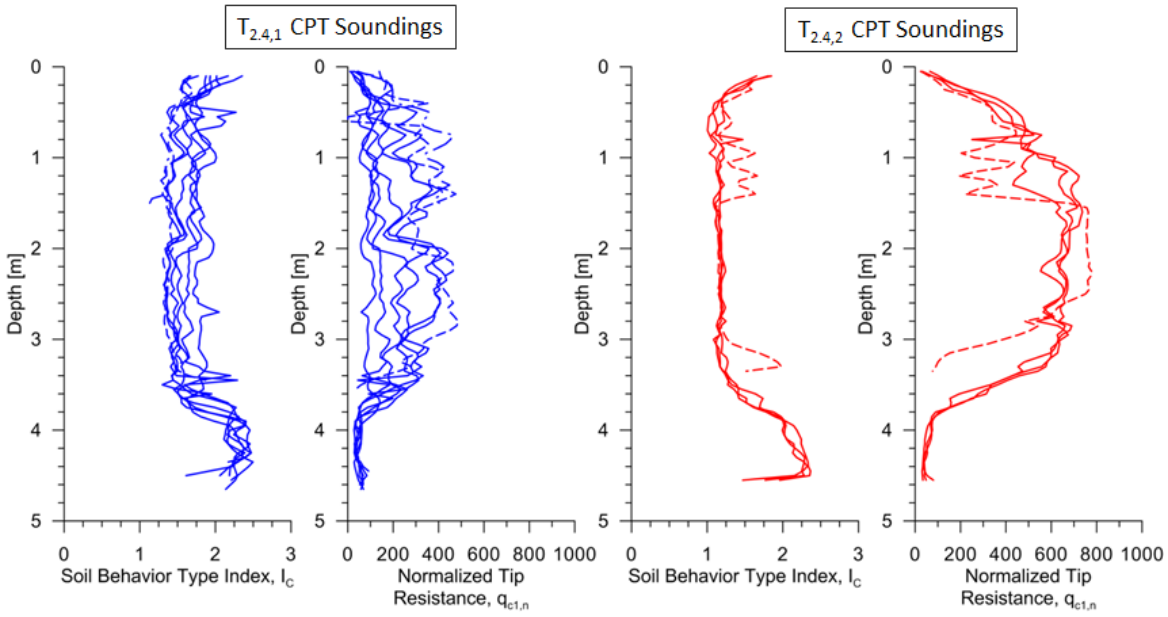

Figure 3.4 CPT data for $T_{2.4,1}$ and $T_{2.4,2}$

Figure 3.4 shows the normalized tip resistance ($q_{c1,N}$) and soil behavior type index (I_c) for the CPT soundings performed for $T_{2.4,1}$ and $T_{2.4,2}$. These quantities are computed using standard procedures as described by Robertson and Wride (1998) and updated by Zhang et al. (2002). Tip resistances from $T_{2.4,1}$ are notably lower than those for $T_{2.4,2}$, suggesting lower overall levels of compaction. As expected, I_c values within the backfill are low (approximately 1.2-1.8), indicating sandy soil.

The $T_{2.4,1}$ data are highly variable both from sounding-to-sounding but also with depth. The depth variations indicate systematic fluctuations over approximately 0.3-0.4 m depth intervals, which we interpret to indicate variable levels of compaction within lift thicknesses. The data do not show systematic changes with depth, which is expected due to the overburden normalization included in the computation of $q_{c1,N}$. The fluctuations between soundings indicate a general level of scatter in the degree of compaction. Tip resistances from $T_{2.4,2}$ are generally more uniform, both between soundings and with depth, indicating relatively uniform compaction within each lift and at different locations within the backfill. Over the depth range of 1.0-3.0 m, average depth-normalized tip resistances for

$T_{2.4,1}$ and $T_{2.4,2}$ are approximately q_{c1N} ≈250 and 500, respectively. These results can be used to estimate relative density using the following empirical correlation (Idriss and Boulanger, 2008):

$$D_r = 0.465\left(\frac{q_{c1N}}{C_{dq}}\right)^{0.264} - 1.063 \tag{3.1}$$

where C_{dq} is an empirical parameter reported to take on values ranging from 0.64 to 1.55 for various sands (Salgado et al., 1997; Idriss and Boulanger, 2008). This correlation produces estimates of D_r of about 1.0 for $T_{2.4,2}$, even for the upper bound value of C_{dq}=1.55. Accordingly, these results corroborate the sand cone tests described above, indicating very high average relative densities in the compacted fill materials. For $T_{2.4,1}$, the reduced q_{c1N} ≈250 causes D_r estimates to be reduced relative to those for q_{c1N} ≈500 by about 0.4 (per Eq 3.1). Good general estimates of D_r for $T_{2.4,1}$ and $T_{2.4,2}$ are 0.6 and 1.0, respectively. As noted previously, these D_r values are expected to be highly variable for $T_{2.4,1}$ and relatively uniform for $T_{2.4,2}$. Soft zones within the backfill for $T_{2.4,1}$ have q_{c1N} ≈100-200, with D_r values possibly in the range of 0.4-0.6. The relative density of $T_{1.68}$ can be estimated as D_r = 0.92 and is likely to range between 0.85 – 1.0.

Soil strength parameters were investigated using triaxial compression tests (ASTM D2850) performed on unsaturated compacted specimens from bulk samples. Each specimen was prepared to achieve a target water content of 9% and a relative compaction level of 96%, which is approximately representative of the compaction condition for $T_{2.4,2.}$ For each specimen, the testing was performed by first placing the specimen under a prescribed cell pressure then shearing the soil to failure by increasing the vertical (deviator) stress. Because the sand specimens are unsaturated, the shearing effectively occurs under drained conditions. The process was repeated for higher cell pressures and the soil tested to failure at each level. These protocols are different from those applied in $T_{1.68}$ (described in Lemnitzer *et. al* 2009) in which the same specimen is used for each confining pressure, which reduces dilatency at the higher confinements. Detailed information on the triaxial tests of $T_{2.4,\ 1\&2}$ can be found in Stewart *et. al* (2011). Stress points for the peak deviator stresses obtained in the triaxial tests for $T_{2.4,2}$ were plotted in *p-q* space as shown in Figure 3.5. These points are used to construct the K_f line, whose equation is expressed as

$$q_f = a + p_f \tan\psi \tag{3.2}$$

A linear regression was performed on the data set to estimate parameters *a* (from the line intercept) and ψ (from the slope of the line) as 20.4 kPa and 29.5°, respectively. The standard deviation of residuals (in the *q* direction) is 9.7 kPa, which translates to a ± one standard deviation range for *a* of 10.7 to 30.1 kPa when holding the slope of the fit line constant. Confidence intervals at the 95% level are also plotted in Figure 3.5. The variability of ψ was evaluated by constructing additional fit lines within the confidence intervals. A lower bound was found by determining the slope of the line that was tangent to the upper interval line at the q-axis and tangent to the lower interval line at the largest *p* value. Similarly, an upper bound estimate of ψ was calculated from the slope of the line tangent to the lower interval line at the q-axis and the upper interval line at the largest *p* value. Using this process, angle ϕ varies between 28.2° and 30.8°.

Once ψ and α are established for the K_f line, strength parameters ϕ and *c* for the Mohr-Coulomb failure envelope can be computed as (e.g., Lambe and Whitman, 1969, *p 141*):

$$\sin\phi = \tan\psi \tag{3.3}$$

$$c = \frac{a}{\cos\phi} \tag{3.4}$$

The resulting envelopes yield a range of friction angle (ϕ) from 32.6° to 36.6° (mean of 34.5° degrees) and range of cohesion (c) from 13.0 and 36.5 kPa, with a mean of 24.8 kPa for $T_{2.4,2}$.

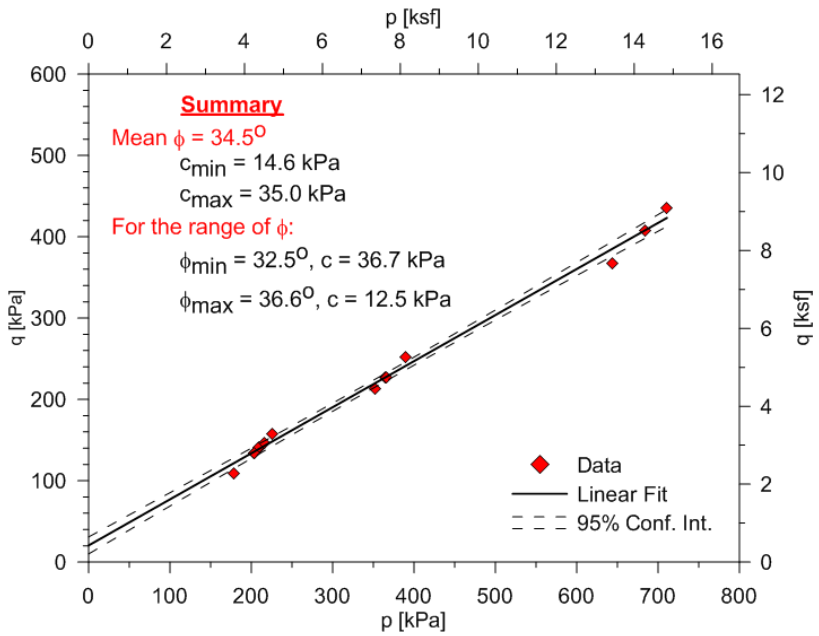

Figure 3. 5 Stress points at failure for various triaxial tests with linear fit of the K_f line ($T_{2.4,2}$). Corresponding parameters for the Mohr-Coulomb failure envelope are reported.

Since the above Mohr-Coulomb parameters represent peak strength conditions for the compaction level of $T_{2.4,2}$, the question rises how parameters would change under different boundary conditions for which laboratory test results are not available. Main concerns relate to the parameter changes due to (1) plane strain conditions, (2) critical state (i.e. residual) conditions and (3) lower compaction conditions such as present in $T_{2.4,1}$. In order to conduct modeling approaches that are able to capture the backfill behavior shown in Figure 2.3, the three issues identified above are discussed as follows and adjustments are applied to the soil strength parameters:

(1) Plane Strain Shear: Lee (1970) describes the higher drained shear strength obtained in plane strain tests as compared to triaxial tests. Friction angles for plane strain conditions are higher than those for triaxial by amounts ranging from 0-8 deg, with the largest differences associated with dense sands and at low confining pressures (i.e., the most dilatent materials). For the conditions present in the SE 30 material used in field testing, a 5 deg offset in ϕ appears reasonable. This changes our mean peak strength parameters to: Mean c= 25 kPa, Mean ϕ=39.5 deg

(2) Critical State Conditions: There are two approaches to this problem. One is to look at the test data, which is not optimal because the tests do not extend to large strain levels typically associated with critical state conditions. Nonetheless, the results of triaxial testing of $T_{2.4,2}$ material suggest an approximate sensitivity (peak/residual strengths) of about 1.2. The reduced friction angle from this approach is ϕ_{cs}=30 deg. Sand materials at critical state would not be expected to have significant curvature in the failure envelopes, so a cohesion of c_{cs}=0 is selected.

This result can be checked against critical state (or residual) friction angles in the literature, which range from 30-35 deg (Negussey et al., 1988). The value identified from the estimate of sensitivity is within this range. In summary, for residual we recommend the following parameters: c_{cs}=0, ϕ_{cs}=30 deg

(3) Lower Compaction Levels: Laboratory testing has not been performed for the lower relative density (D_r) conditions that appear to have been present in $T_{2.4,1}$. Residual strengths will not change for

the lower compaction levels, but peak strengths will decrease. Bolton (1986) found a relationship between relative state parameter index (I_{RD}) and difference between peak and critical state friction angles as:

$$\phi - \phi_{cs} = xI_{RD} \tag{3.5}$$

where x is approximately 3 for triaxial and 5 for plane strain. For the present set of test data, we calculate ϕ-ϕ_{cs} = 9.5 deg. Parameter I_{RD} is computed as (Bolton, 1986):

$$I_{RD} = D_r\left(Q - \ln\frac{100p'}{p_a}\right) - R \tag{3.6}$$

where $Q \approx 10$ (quartz and feldspar), $R \approx 1.0$, p' = mean stress at failure, p_a = reference stress of 100 kPa. Using stresses for a representative depth of 2.5 m in Eq. (3.6) with a D_r range of 0.85 – 1.0 gives I_{RD} = 4 to 5. Using this value of I_{RD} in Eq. (3.5) indicates that x = 2 – 2.5.

The reduced D_r of 0.4 – 0.6 for $T_{2.4,1}$ can be entered into Eq. (3.6) to find I_{RD} = 1.4 – 2.7, which translates to ϕ-ϕ_{cs} = 3 – 6 deg per Eq. (3.5) with the range of x identified above. Hence, for the looser specimen, peak friction angles are estimated to be in the range of 33 to 36 deg (for plane strain). The cohesion associated with this friction angle is unknown, but a lower value than was used for the high D_r backfill is considered appropriate due to reduced dilatency (less curvature of failure surface). The estimated cohesion for this case is in the range of 10 – 15 kPa.

4. MODELLING STUDIES

Using the strength parameters identified above, numerical modeling was conducted using the log spiral hyperbolic (LSH) simulation procedure by Shamsabadi et al (2010) to capture the trends of the load displacement relationships presented in Figure 2.3. The model implemented the wall dimensions given in Section 2 of this paper, a soil unit weight of 20.1 kN/m^3, ε_{50}=0.35%, failure ratio R_f = 0.97, the strength parameters given in the prior section, and a wall-soil interface friction angle of δ=0.5ϕ (using peak strengths for ϕ). LSH simulations were performed for specimens $T_{2.4,1}$ and $T_{2.4,2}$. With results given in Figures 4.1-4.2. The simulations are able to capture the large differences between peak strengths in the two tests, suggesting that the different compaction levels are responsible for the different levels of measured passive capacity.

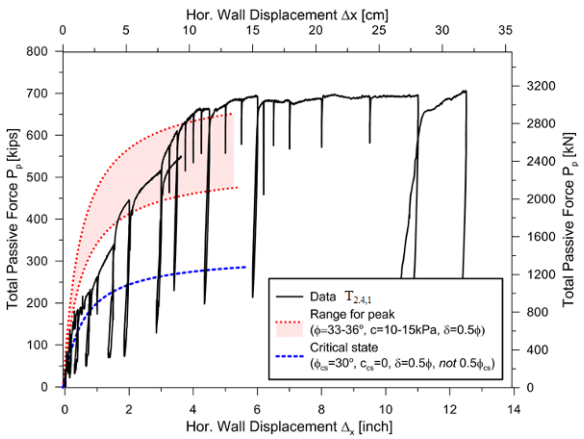

Figure 4.1. Test results for $T_{2.4,1}$ and LSH predictions of capacity using suggested strength parameters

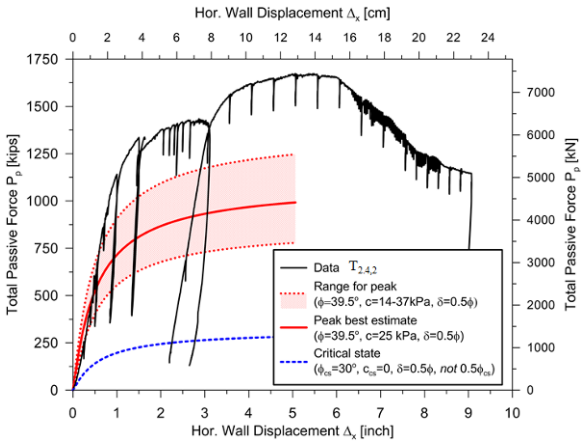

Figure 4.2. Test results for $T_{2.4,1}$ and LSH predictions of capacity using suggested strength parameters

For test $T_{2.4,1}$, the LSH simulation using peak strength parameter overestimate initial stiffness and underestimate peak strength, although the upper bound of considered range is close to the peak strength. The simulations using critical state strengths underpredict stiffness and significantly underestimate capacity. It appears that the assumption of zero cohesion for the critical state condition may be too conservative.

For test $T_{2.4,2}$, the LSH simulation using peak strength parameter capture well the initial stiffness and underestimate peak strength, although the upper bound of considered range is close to the peak strength. The 'best estimate' parameters for the peak strength come close to predicting the resistance at the largest deformation levels (approaching residual). As before, the simulations using critical state strengths underpredict stiffness and significantly underestimate capacity. It appears that the assumption of zero cohesion for the critical state condition may be too conservative.

For both $T_{2.4}$ tests, the upper bound of the considered range in strength parameters provides wall resistances that are low by amounts ranging from about 15-25%. The center of the range is low by amounts ranging from 30-70%. However, while the predictions are somewhat low, they do capture the large change in resistance between $T_{2.4,1}$ and $T_{2.4,2}$ resulting from the different compaction conditions. Several factors may contribute to the LSH under-predictions of peak resistance for the $T_{2.4}$ tests. The offset between triaxial and plane strain shear strengths may be higher than anticipated and may also affect cohesion (we only adjusted friction angle). Moreover, the laboratory test specimens may not exactly match field conditions due to subtle differences in compaction methods (less grain breakage in lab) and due to ageing effects that are present in the field but not in the lab tests (e.g., Mitchell and Soga, 2005, p513).

5. SUMMARY AND CONCLUSION

An abutment backwall system with granular backfill material of heights 1.68m and 2.4m was subjected to quasi static lateral loading. Two separate tests were performed on a 2.4m backfill height specimen, which has been compacted in the field with different compaction methods, while all other boundary conditions were identical during the experiment construction and conduction.

The lower level compacted sandy backfill revealed insitu relative densities ranging from approximately D_r = 0.4-0.6 in specimen 1 to unusually high levels of compaction of D_r = 0.9-1.0 in specimen 2 leading to significant differences of approximately 50% in initial stiffness and ultimate capacity in the passive load-displacement relationship. Soil strength parameters were determined using drained triaxial testing over a range of normal stresses that represent in situ conditions. Peak strength parameters were evaluated for the dense backfill configuration (specimen 2) and corrections applied for plane strain effects and for the looser backfill configuration (specimen 1). Analytical simulations of the backfill response were conducted using the LSH method, and modest under prediction of the peak response for the upper bound of the considered range of strengths was identified. Central values of strength parameters produce more substantial under prediction. Nonetheless, the degree of underprediction is modest relative to the substantial differences in capacity between both specimens and the analytical model can capture the differences in soil strength parameters sufficiently.

ACKNOWLEDGEMENTS

Support for this research was provided by the California Department of Transportation under Research Contract No. 59A0247 and amendments thereto, which is gratefully acknowledged. The authors would like to acknowledge the valuable assistance and technical support of Caltrans staff in this project, particularly Li-Hong Sheng. George Cooke of GB Cooke Inc. is recognized for his assistance in specimen construction and contract administration. Partial support for the testing phase of this project was also provided through the George E. Brown, Jr. Network for Earthquake Engineering Simulation _NEES_ Program of the National Science Foundation under Award No. CMMI-0402490. The writers gratefully acknowledge the contributions of the NEES@ UCLA Equipment site, and particularly thank Steve Keowen, Alberto Salamanca and Steve Kang for their important contributions associated with the timely and effective completion of the testing.

REFERENCES

ASTM. (2009). "Standard Test Methods for Laboratory Compaction Characteristics of Soil Using Modified Effort (56,000 ft-lbf/ft^3 (2,700 kN-m/m^3))." *D1557*, West Conshohoken, Pa.

ASTM. (2006). "Standard Test Methods for Maximum Index Density and Unit Weight of Soils Using a Vibratory Table." *D4253*, West Conshohoken, Pa.

ASTM. (2006). "Standard Test Methods for Minimum Index Density and Unit Weight of Soils and Calculation of Relative Density" *D4254*, West Conshohoken, Pa.

ASTM. (2007). "Standard Test Method for Unconsolidated-Undrained Triaxial Compression Test on Cohesive Soils." *D2850*, West Conshohoken, Pa.

Bolton, M.D. (1986). "The strength and dilatancy of sands." *Geotechnique*, 36 (1), 65-78.

California Dept. of Transportation (CALTRANS). (2010). "Seismic Design Criteria, ver.1.6, Nov 2010." *CALTRANS*, Division of Engineering Services, Office of Structure Design,Sacramento,Calif.,http://www.dot.ca.gov/hq/esc/earthquake_engineering/SDC_site/2010-11-17_SDC_1.6_Full_Version_OEE_Release.pdf

Idriss, I.M., and Boulanger, R.W. (2008). *Soil Liquefaction During Earthquakes*, Monograph series, No. MNO-12, Earthquake Engineering Research Institute.

Lambe, T. W., and Whitman, R. V. (1969). *Soil Mechanics*, Wiley and Sons, NY.

Lee, KL (1970). "Comparison of plane strain and triaxial tests on sand," *J. Soil Mechanics & Foundations Div.*, ASCE, 96 (3), 901-923.

Lemnitzer, A., Ahlberg, E.R., Nigbor, R.L., Shamsabadi, A., Wallace, J.W., and Stewart, J.P. (2009). "Lateral performance of full-scale bridge abutment wall with granular backfill" *J.Geotech. & Geoenv. Eng.*, ASCE, 135 (4), 506-514.

Mitchell, J.K., and Soga, K., (2005). *Fundamentals of Soil Behavior*, 3rd Edition. John Wiley & Sons, Hoboken.

Negussey, D., Wijewickreme, W.K.D., and Vaid, Y .P. (1988). Constant volume friction angle of granular materials. Canadian Geotechnical Journal, **25:** 50-55.

Robertson, P.K., and Wride, C.E. (1998). "Evaluating cyclic liquefaction potential using the cone penetration test." *Can. Geotech. J.* **35**: 442–459.

Rollins, K. M., and Cole, R. T. (2006). "Cyclic lateral load behavior of a pile cap and backfill." *J. Geotech. Geoenviron. Eng.*, ASCE 132 (9), 1143–1153.

Romstadt, K., Kutter, B.L, Maroney, B., Vanderbilt, E., Griggs, M., and Chai, Y.H. (1995). "Experimental measurements of bridge abutment behavior." *Rep. No UCD-STR-95-1*, Structural Engineering Group, Univ. of California, Davis, CA.

Salgado, R., Mitchell, J. K., and Jamiolkowski, M. (1997). "Cavity Expansion and Penetration Resistance in Sand." *J. Geotech. & Geoenv. Eng.*, ASCE, 123 (4), 344-354.

Shamsabadi, A., Rollins, K.M., and Kapuskar, M. (2007). "Nonlinear soil-abutment-bridge structure interaction for seismic performance based design." *J. Geotech. Geoenviron. Eng.*, ASCE, 133 (6), 707–720.

Shamsabadi, A., Khalili-Tehrani, P. Stewart, J.P., Taciroglu, E. (2010). "Validated simulation models for lateral response of bridge abutments with typical backfills." *J. Bridge Eng.*, ASCE, 15 (3), 302-312.

Stewart, J.P., E. Taciroglu, J.W. Wallace, A. Lemnitzer, C. Hilson, A. Nojuomi, S. Keowen, R.L. Nigbor, and A. Salamanca (2011). "Nonlinear load-deflection behavior of abutment backwalls with varying height and soil density" *Report No. UCLA-SGEL 2011/01*, Structural and Geotechnical Engineering Laboratory, University of California, Los Angeles.

Zhang, G., Robertson, P. K., and Brachman, R. W. I. (2002). "Estimating liquefaction induced ground settlements from CPT for level ground." *Can. Geotech. J.*, 39 (5), 1168–1180.